

## Article

# Simulation of the Ozone Concentration in Three Regions of Xinjiang, China, Using a Genetic Algorithm-Optimized BP Neural Network Model

Qilong Zhao <sup>1</sup>, Kui Jiang <sup>2</sup> , Dilinuer Talifu <sup>1,\*</sup> , Bo Gao <sup>3</sup> , Xinming Wang <sup>4,5</sup> , Abulikemu Abulizi <sup>1</sup>, Xiaohui Zhang <sup>1</sup> and Bowen Liu <sup>1</sup>

<sup>1</sup> Xinjiang Key Laboratory of Coal Clean Conversion and Chemical Engineering, College of Chemical Engineering, Xinjiang University, Urumqi 830017, China

<sup>2</sup> National Engineering Research Center for Multimedia Software, School of Computer Science, Wuhan University, Wuhan 430072, China

<sup>3</sup> Guangdong Provincial Key Laboratory of Water and Air Pollution Control, South China Institute of Environmental Science, Ministry of Ecology and Environment, Guangzhou 510655, China

<sup>4</sup> State Key Laboratory of Organic Geochemistry, Guangzhou Institute of Geochemistry, Chinese Academy of Sciences, Guangzhou 510640, China

<sup>5</sup> Guangdong-Hong Kong-Macao Joint Laboratory for Environmental Pollution and Control, Guangzhou Institute of Geochemistry, Chinese Academy of Sciences, Guangzhou 510640, China

\* Correspondence: dilnurt@xju.edu.cn

**Abstract:** Accurate ozone concentration simulation can provide a health reference for people's daily lives. Simulating ozone concentrations is a complex task because near-surface ozone production is determined by a combination of volatile organic compounds (VOCs) and NO<sub>x</sub> emissions, atmospheric photochemical reactions, and meteorological factors. In this study, we applied a genetic algorithm-optimized back propagation (GA-BP) neural network, multiple linear regression (MLR), BP neural network, random forest (RF) algorithm, and long short-term memory network (LSTM) to model ozone concentrations in three regions of Xinjiang, China (Urumqi, Hotan, and Dushanzi districts) for the first time by inputting wind speed, humidity, visibility, temperature, and wind direction. The results showed that the average relative errors of the model simulations in the Urumqi, Hotan, and Dushanzi districts were BP (61%, 14%, and 16%), MLR (97%, 14%, and 23%), RF (39%, 11%, and 14%), LSTM (50%, 12%, and 16%), and GA-BP (16%, 4%, and 6%) and that the significance coefficients R<sup>2</sup> were BP (0.73, 0.65, and 0.83), MLR (0.68, 0.62, and 0.74), RF (0.85, 0.80, and 0.88), LSTM (0.78, 0.74, and 0.85), and GA-BP (0.92, 0.93, and 0.94), respectively, with the simulated values of GA-BP being the closest to the true values. The GA-BP model results showed that among the 100 samples with the same wind speed, humidity, visibility, temperature, and wind direction data, the highest simulated ozone concentrations in the Urumqi, Hotan, and Dushanzi districts were 173.5 μg/m<sup>3</sup>, 114.3 μg/m<sup>3</sup>, and 228.4 μg/m<sup>3</sup>, respectively. The results provide a theoretical basis for the effective control of regional ozone pollution in urban areas (Urumqi), dusty areas (Hotan), and industrial areas (Dushanzi) in Xinjiang.

**Keywords:** meteorological factors; atmospheric conditions; ozone concentration; genetic algorithm; BP neural network; Xinjiang region



**Citation:** Zhao, Q.; Jiang, K.; Talifu, D.; Gao, B.; Wang, X.; Abulizi, A.; Zhang, X.; Liu, B. Simulation of the Ozone Concentration in Three Regions of Xinjiang, China, Using a Genetic Algorithm-Optimized BP Neural Network Model. *Atmosphere* **2023**, *14*, 160. <https://doi.org/10.3390/atmos14010160>

Academic Editors:

Chandrasekar Radhakrishnan,  
Haonan Chen and V. Chandrasekar

Received: 29 November 2022

Revised: 2 January 2023

Accepted: 7 January 2023

Published: 11 January 2023



**Copyright:** © 2023 by the authors. Licensee MDPI, Basel, Switzerland. This article is an open access article distributed under the terms and conditions of the Creative Commons Attribution (CC BY) license (<https://creativecommons.org/licenses/by/4.0/>).

## 1. Introduction

The air quality index (AQI) in China is composed of six indexes: sulfur dioxide (SO<sub>2</sub>), inhalable particulate matter (PM<sub>10</sub>), ozone (O<sub>3</sub>), fine particulate matter (PM<sub>2.5</sub>), carbon monoxide (CO), and nitrogen dioxide (NO<sub>2</sub>). Among these, ozone (O<sub>3</sub>) and particulate matter (PM) are significant air pollutants that negatively affect the Earth's ecology, global climate, and human health [1–6]. In recent years, with the strengthening of China's air quality management, although the concentration of PM<sub>2.5</sub> in cities has achieved a significant

decrease, the concentration of O<sub>3</sub> has increased dramatically. Ozone has replaced PM<sub>2.5</sub> as the major air pollutant in some Chinese regions [7–9]. Ozone, which is concentrated in the stratosphere, protects life on Earth by blocking some of the high-intensity ultraviolet radiation that reaches the surface and by absorbing the solar short-wave radiation that is harmful to humans and other organisms. However, a small portion of ozone in the troposphere becomes greenhouse gases and atmospheric pollutants [10]. A high concentration of ozone near the ground will not only affect the atmospheric environment but also cause harm to human health [2,11–14]. Ozone is a strong oxidizer and plays an important role in atmospheric chemistry and climate change, being the third most important greenhouse gas after methane and carbon dioxide [15,16]. In terms of human health effects, ozone can cause local chronic inflammation of the respiratory system [1], damage human health systems, and accelerate human aging [3]. Vulnerable populations (pregnant women, infants, etc.) even face the risk of death if they are exposed to high ozone concentrations for long periods [17].

Most of the ozone near the surface is produced by complex photochemical reactions from its precursors, such as volatile organic compounds (VOCs) and nitrogen oxides (NO<sub>x</sub>) [9,18–20]. The formation of ozone is a highly nonlinear process [19,21–23]. Therefore, the simple line model in existing methods is far from satisfying the real-world requirement. In addition, meteorological factors and complex weather models greatly increase the difficulty of simulating ozone concentrations [24].

In recent years, artificial neural networks have attracted increasing attention due to their impressive nonlinear processing power and fault tolerance in modeling pollutant concentrations, thus offering new solutions to air pollution problems. These methods show better simulation results in the field of urban air quality simulation than traditional methods [25–29]. Wan et al. [30] introduced a common single implicit layer artificial BP neural network to simulate the ozone concentration in Dalian. The results show that the simulation model established by the artificial neural network has generalization ability, strong versatility, and objectivity and has the value of the practical application. Jia Xing et al. [31] developed a deep learning model using an LSTM neural network-based model to simulate ozone concentrations using the CMAQ model. By inputting six meteorological variables, and one topographic height variable, the most severe ozone pollutions in three key regions in the North China Plain, the Yangtze River Delta, and the Pearl River Delta were simulated. The ozone simulation model they developed has a great potential for accurately and efficiently describing ozone concentrations in the intricate atmospheric system. Government environmentalists can use it as a basis to design effective emission reduction methods to reduce ozone pollution. Yong Cheng et al. [32] accurately simulated ozone concentrations in six megacities in China using a hybrid model that combines neural networks and wavelet decomposition algorithms. In their study, the average R<sup>2</sup> of the hybrid model was 0.95, which can be considered a very good result for a model. The results show that the neural network can provide a technical reference for near-surface ozone estimation, which has important practical implications for ozone concentration monitoring. Sun-Kyong et al. [33] used a neural network model based on weather patterns quantified in the form of cosine similarity as a predictor to train the neural network model for the predictability assessment of four PM<sub>10</sub> grades in Seoul, Korea. The results show that the predictability assessment obtained from the neural network model is reliable and can be used as a statistical reference for current air quality prediction systems. Fabio et al. [34] compared multiple linear regression models and neural network models with and without a recursive structure for predicting daily average PM<sub>10</sub> concentrations for the next from one to three days. The results showed that the neural network model with a recursive structure was the best performer among the three models and that the recurrent artificial neural network can be used as a powerful operational tool for predicting particulate matter concentrations. Ebrahim et al. [35] used a deep convolutional neural network to predict hourly ozone concentrations in Seoul in 2017 by inputting wind fields, temperature, relative humidity, barometric pressure, and precipitation, as well as ozone and NO<sub>2</sub> concentrations. The results showed that although

the deep convolutional neural network has some limitations, it can still successfully capture the daily trends of ozone concentrations and the high and low changes in concentrations from year to year. More and more new algorithmic optimization models are being applied to agriculture and the environment, such as the hybrid extreme learning machine combined with hybrid particle swarm optimization and grey wolf optimization (ELM-PSOGWO) [36], the hybrid support vector regression with the simulated annealing algorithm and the mayfly optimization algorithm (SVR-SAMOA) [37], and the hybrid adaptive neuro-fuzzy system and the gradient-based optimization (ANFIS-GBO) [38].

The genetic algorithm (GA), a well-known ML algorithm inspired by the natural selection processes in biology [39], is a robust and effective technology for solving multi-objective optimization problems [40]. The GA has been widely used in environmental management and engineering [41,42] and has been successfully applied in designing ozone control strategies [43]. Therefore, this study uses a BP neural network optimized by the genetic algorithm to solve the problems of undertraining or overfitting that occur during the training of ordinary BP neural networks. Using this method, the connection weights and thresholds of the BP neural network can be trained and optimized, which has a positive effect on further improving the simulation ability of BP neural networks.

The air qualities of the cities in Xinjiang are affected by many factors such as geographical location, natural environment, energy structure, and economic development, which directly or indirectly affect the development of the cities and the health of the citizens. Therefore, it is important to study the air quality of the cities for the development of the Xinjiang region and human health. Zhang et al. [44] investigated the chemical composition and source characteristics of PM<sub>2.5</sub> in Urumqi, Xinjiang and found that relative humidity played a key role in influencing visibility and that residential coal combustion and vehicle emissions were the main sources of air pollution. Turap et al. [45] studied the chemical composition and source characteristics of PM<sub>2.5</sub> in Dushanzi District, Xinjiang and the results showed that the highest average PM<sub>2.5</sub> concentrations were found in the Dushanzi District in winter and that the contribution of the source has significant seasonal changes. Liu et al. [46] found for the first time that the  $\alpha$ -SiO<sub>2</sub> concentration in PM<sub>2.5</sub> influenced the atmospheric visibility in the urban area of Hotan, Xinjiang and the presence of oasis could effectively reduce the  $\alpha$ -SiO<sub>2</sub> concentration.

In summary, the previous studies have the following shortcomings: (1) there were many studies on particulate matter pollution in Xinjiang but few studies have simulated ozone pollution in Xinjiang using BP neural networks optimized with genetic algorithms; (2) the extremely complex atmospheric composition, unique arid climatic conditions, and industrial environment of the Xinjiang region cause it to be difficult for traditional fitting methods to meet the requirements of precise ozone concentration prediction; and (3) existing studies exploring urban air pollution levels in Xinjiang were limited to the urban areas and contained few cases on air pollution levels in multiple cities.

In this study, we applied GA-BP, BP, MLR, RF, and LSTM models by inputting wind speed, humidity, visibility, temperature, and wind direction to model ozone concentrations in urban (Urumqi city), dusty (Hotan city), and industrial (Dushanzi district) areas of Xinjiang, China for the first time and simulated the ozone pollution conditions in each region under the same wind speed, humidity, visibility, temperature, and wind direction conditions.

## 2. Materials and Methods

### 2.1. Research Area Location

The Xinjiang Uygur Autonomous Region of China is located between longitude 73°40′96″18″ East and latitude 34°25′48″10′ North. Xinjiang covers the largest area of China's 34 provincial-level administrative regions and it accounts for about one-sixth of the country's total territorial area. Because of the vast area of Xinjiang, urban development has unique characteristics. The three cities in this study have distinct characteristics, among which Urumqi City is a typical urban area in Xinjiang, Hotan City is a typical wind-sand area in Xinjiang, and Dushanzi District is a typical petrochemical industrial area in Xinjiang.

The area map of the research location is shown in Figure 1. Urumqi city, Hotan city, and Dushanzi district represent three typical regions in Xinjiang: an urban area, dusty area, and industrial area, respectively. The brief characteristics of the three regions are shown in Table S1.

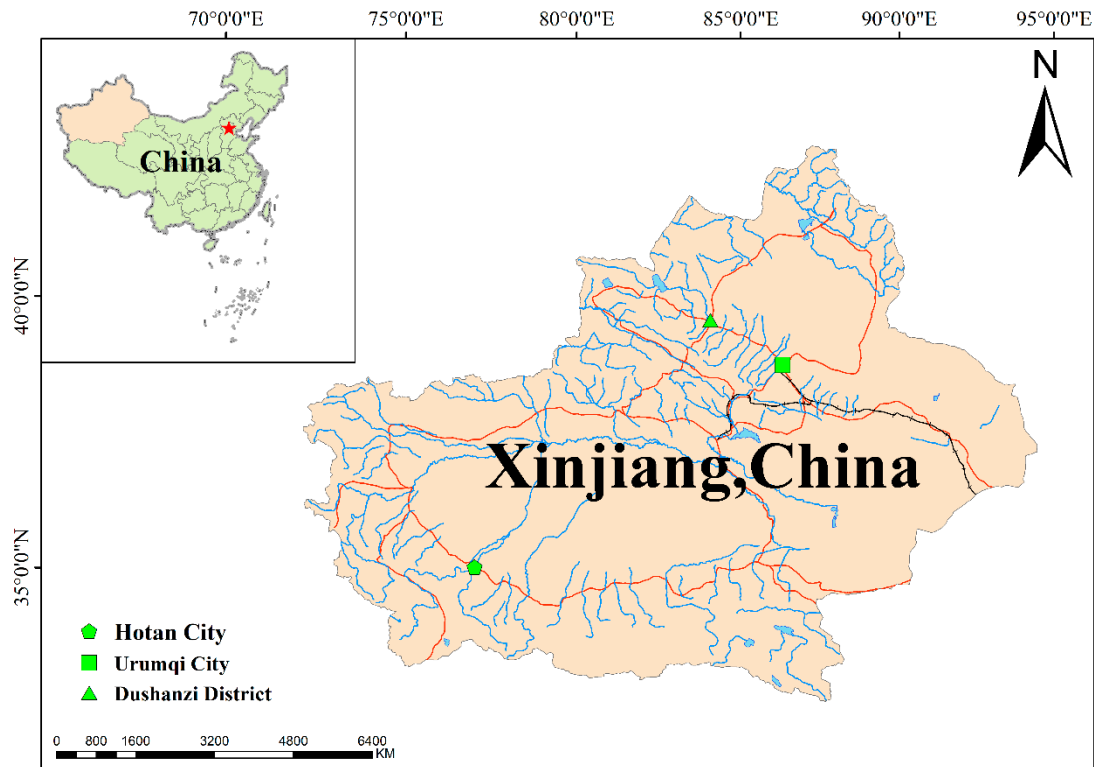


**Figure 1.** The geographical locations of Urumqi City, Hotan City, and Dushanzi District.

## 2.2. Data Classification and Source

In this study, 50 sets of data were collected from Urumqi, Hotan, and Dushanzi districts and a total of 150 sets of data were used for model training. The data on meteorological factors, atmospheric conditions, and ozone concentrations for Urumqi were obtained from the Internet (<https://map.zq12369.com/>, accessed on 25 November 2022; <https://rp5.ru/>, accessed on 25 November 2022) and data for Hotan City and the Dushanzi Region were provided by local environmental protection authorities.

## 2.3. Establishment of the Ozone Concentration Model

The process of ozone formation is very complex. The effects of various meteorological factors, atmospheric conditions, and precursor emissions on ozone production are interrelated. In this study, we trained three GA-BP neural network models based on the MATLAB platform to simulate ozone concentration values using data from five meteorological elements and atmospheric conditions in weather forecasts. A large amount of data were used to simulate the relationship between data on the five meteorological factors, atmospheric conditions, and ozone concentration data at the same time and this relationship was used to estimate the current ozone concentration. The specific input layer data and output layer data are shown in Table 1. In Section 3.4 of this study, we compare the simulation results of GA-BP with those of the ordinary BP neural network model (BP), the traditional multiple linear regression model (MLR), random forest model (RF), and long short-term memory neural network model (LSTM). BP neural networks are vulnerable to the problem of a local minimum [47], which immensely weakens the regression ability of the BP neural network and leads to a lower forecast accuracy. The genetic algorithm can optimize the weights and thresholds of the BP neural network, so the simulation performance of a GA-BP neural

network is better than that of an ordinary BP neural network [48]. At present, GA-BP neural networks have been applied in many disciplines [49,50]. In most studies [31,48,51,52], other atmospheric pollutants such as the NO<sub>x</sub> concentration, particulate matter concentration, and meteorological conditions are used as input parameters. In order to simulate the ozone concentrations quickly and easily, only five meteorological conditions were used as input parameters in this study. The study used the input and output methods of the model, as shown in Table 1.

**Table 1.** Specific input and output information of the model.

	Name	Unit
Input	Temperature	°C
	Relative Humidity	%
	Wind direction	°
	Wind Speed	m/s
	Visibility	Km
Output	O <sub>3</sub> concentration	µg/m <sup>3</sup>

The input data (temperature, humidity, wind direction, wind speed, and visibility) used to train the model in the three regions were selected randomly for a certain time period. The model training set for Urumqi city used data from June to July, from November to December 2020, and from March to April 2021. The training set of the Hotan city model used the data of January and July 2020. The model training set for the Dushanzi District used data from December 2015 to April–May 2016.

The number of implied layer nodes was selected using an automatic optimization-seeking algorithm, which automatically selected the number of implied layer nodes with the smallest error by comparing various implied layer nodes within a certain range and, after the selection and comparison, the number of implied layer nodes for the models in Urumqi, Hotan, and Dushanzi districts were 5, 10, and 12, respectively. In all three regions, the single hidden layer GA-BP neural network model had an R<sup>2</sup> above 0.91 and the other performance indexes were much higher than the other four models that have met the requirements of ozone simulation. Therefore, this research team used the BP neural network model with a single hidden layer for ozone simulation. The comparison process is shown in Table 2. The structure of the BP neural network in this study is shown in Figure 2.

**Table 2.** The process of determining the number of nodes in the implicit layer.

Number of Nodes in the Hidden Layer	Urumqi	Hotan	Dushanzi
	Mean Square Error	Mean Square Error	Mean Square Error
3	$6.0 \times 10^{-4}$	$2.9 \times 10^{-4}$	$2.9 \times 10^{-4}$
4	$4.3 \times 10^{-4}$	$1.5 \times 10^{-4}$	$4.0 \times 10^{-4}$
5	$7.4 \times 10^{-5}$	$1.9 \times 10^{-4}$	$4.3 \times 10^{-4}$
6	$1.9 \times 10^{-4}$	$1.4 \times 10^{-4}$	$2.4 \times 10^{-4}$
7	$3.0 \times 10^{-4}$	$2.0 \times 10^{-4}$	$5.3 \times 10^{-4}$
8	$1.3 \times 10^{-4}$	$1.9 \times 10^{-4}$	$3.3 \times 10^{-4}$
9	$1.2 \times 10^{-4}$	$1.7 \times 10^{-4}$	$4.1 \times 10^{-4}$
10	$1.5 \times 10^{-4}$	$1.2 \times 10^{-4}$	$3.7 \times 10^{-4}$
11	$2.6 \times 10^{-4}$	$1.6 \times 10^{-4}$	$2.2 \times 10^{-4}$
12	$1.1 \times 10^{-4}$	$1.3 \times 10^{-4}$	$2.1 \times 10^{-4}$

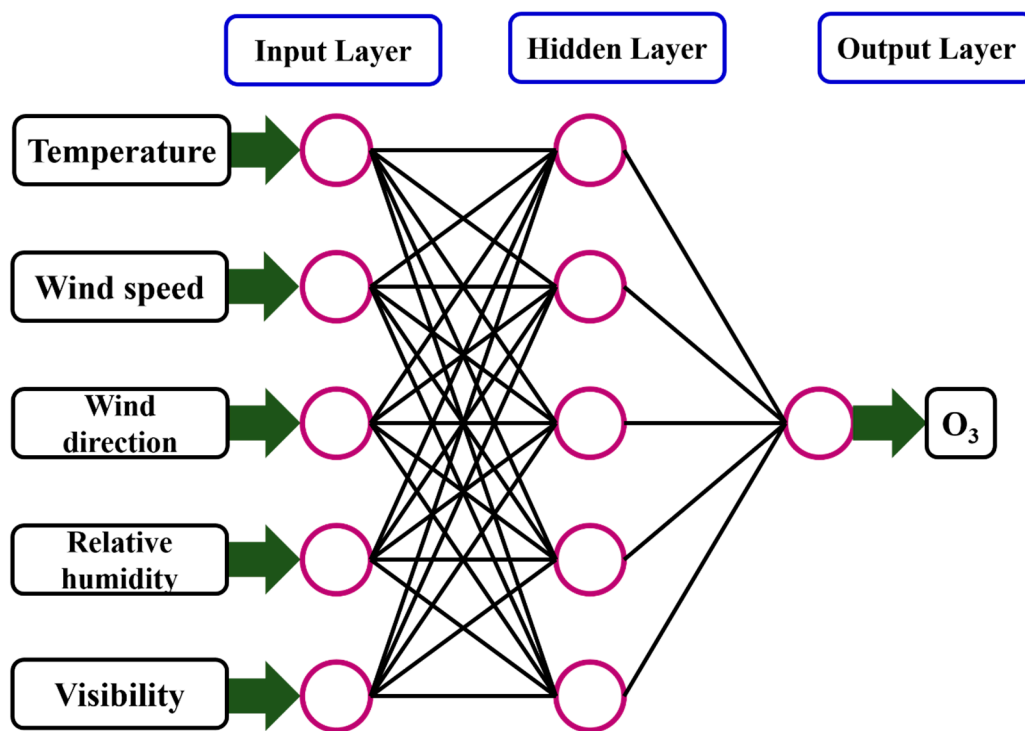


Figure 2. The framework of the ozone simulation model.

In this study, the process of optimizing the BP neural network used a genetic algorithm. The individuals of the population contained the weights and thresholds of each layer of the neural network, the corresponding individual fitness within the individual was calculated according to the designed fitness function, and then the individuals with the best fitness were determined through the operations of selection, crossover, and variation [53]. The optimization process is shown in Figure 3. The neural network model optimized by the genetic algorithm can simulate the ozone concentration at that time by inputting the data of five meteorological factors and atmospheric conditions data. When the ozone concentration exceeds the limit value of the national standard, an early warning can be issued to remind people to minimize going outside and to stay indoors as much as possible, thus reducing the ozone hazard to humans. After several experimental comparisons, the hyperparameters of the model were set as shown in Table 3.

Table 3. Hyperparameter setting of the model.

Training Parameters	Settings
Number of training sessions	net1.trainParam.epochs = 1000
Learning Rate	net1.trainParam.lr = 0.01
Minimum error of training target	net1.trainParam.goal = 0.00001
Display frequency	net1.trainParam.show = 25
Momentum factor	net1.trainParam.mc = 0.01
Minimum performance gradient	net1.trainParam.min_grad = $1 \times 10^{-6}$
Maximum number of failures	net1.trainParam.max_fail = 6
Initial population size	PopulationSize_Data = 30
Maximum number of evolutionary generations	MaxGenerations_Data = 50
Crossover probability	CrossoverFraction_Data = 0.8
Mutation probability	MigrationFraction_Data = 0.2

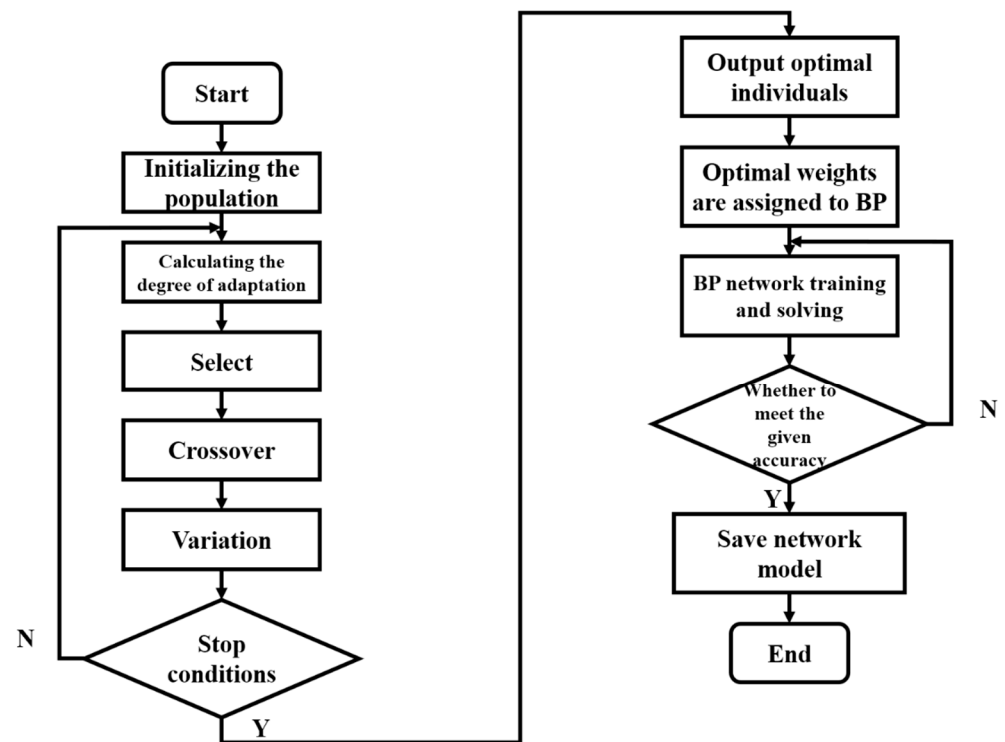


Figure 3. Genetic algorithm optimization process.

The tan-sigmoid function is used as the transfer function. When the input value of the tan-sigmoid function is in the interval  $[-1, 1]$ , it is more sensitive. If the input value is close to or beyond this interval, the function will lose its sensitivity and enter the saturation state, thus affecting the simulation accuracy of the network [54].

However, this study did not select the data normalization processing method often used in other studies [55].

$$X = \frac{X_i - X_{\min}}{X_{\max} - X_{\min}} \tag{1}$$

Although this method is feasible and effective, if it is applied in practice, it is impossible to carry out inverse normalization without known maximum and minimum values, which causes it to be difficult for future practical application. Therefore, this study adopted the following method for data normalization.

For temperature, humidity, and visibility data:

$$y_j = x_j \times 10^{-2} \tag{2}$$

For wind speed data:

$$y_j = x_j \times 10^{-1} \tag{3}$$

For wind direction and ozone concentration data:

$$y_j = x_j \times 10^{-3} \tag{4}$$

In the above formula, “ $y_j$ ” represents the normalized data and “ $x_j$ ” represents the original data. This method can also process raw data between 0 and 1 and is convenient for practical application. We put normalized wind velocity, humidity, visibility, temperature, and wind direction data into the GA-BP neural network model. After the model in this study was trained, the ozone concentration value could be the output as designed.

#### 2.4. Performance Metrics

In this study, the performance of the model was evaluated by five indicators:  $R^2$ , MAE, MSE, RMSE, and NRMSE. Their formulas are as follows [56].  $O_i$  represents the observed true value and  $P_i$  represents the simulated value.

Coefficient of determination ( $R^2$ ):

$$R^2 = 1 - \frac{\sum_{i=1}^n (O_i - P_i)^2}{\sum_{i=1}^n (O_i - O_m)^2} \quad 0 \leq R^2 \leq 1 \quad (5)$$

Mean Absolute Error (MAE):

$$MAE = \frac{1}{n} \sum_{i=1}^n |O_i - P_i| \quad (6)$$

Mean Square Error (MSE):

$$MSE = \frac{1}{n} \sum_{i=1}^n (O_i - P_i)^2 \quad (7)$$

Root Mean Square Error (RMSE):

$$RMSE = \sqrt{\frac{1}{n} \sum_{i=1}^n (O_i - P_i)^2} \quad (8)$$

Normalized Root Mean Square Error (NRMSE):

$$NRMSE = \frac{\sqrt{\frac{1}{n} \sum_{i=1}^n (O_i - P_i)^2}}{O_{\max} - O_{\min}} \quad (9)$$

### 3. Results and Discussion

The three GA-BP neural network models were used to forecast the ozone concentration in Urumqi City, Hotan City, and Dushanzi District. The simulated results were as follows.

#### 3.1. Results of the Ozone Concentration in Urumqi City

As can be seen from Table S2, the ozone simulation model of Urumqi City based on the GA-BP neural network had a minimum relative error of  $2 \times 10^{-3}\%$  and a maximum of 112.7% after simulating the ozone concentration of 50-day samples in this area. The minimum absolute error was  $9.87 \times 10^{-5}$ , the maximum was 27.2, and the mean was 4.259326. Among them, the relative error was less than 30% for 44 days and greater than 50% for 5 days, accounting for 88% and 10%, respectively. The linear fitting results of the real value and simulated value of the ozone simulation model in Urumqi City are shown in Figure 4d. The coefficient of determination for the linear fit between the real ozone concentration value and the simulated ozone concentration value was  $R^2 = 0.918$ . Figure 4a shows the comparison result of the ozone concentration value simulated by the Urumqi model and the real ozone concentration value.

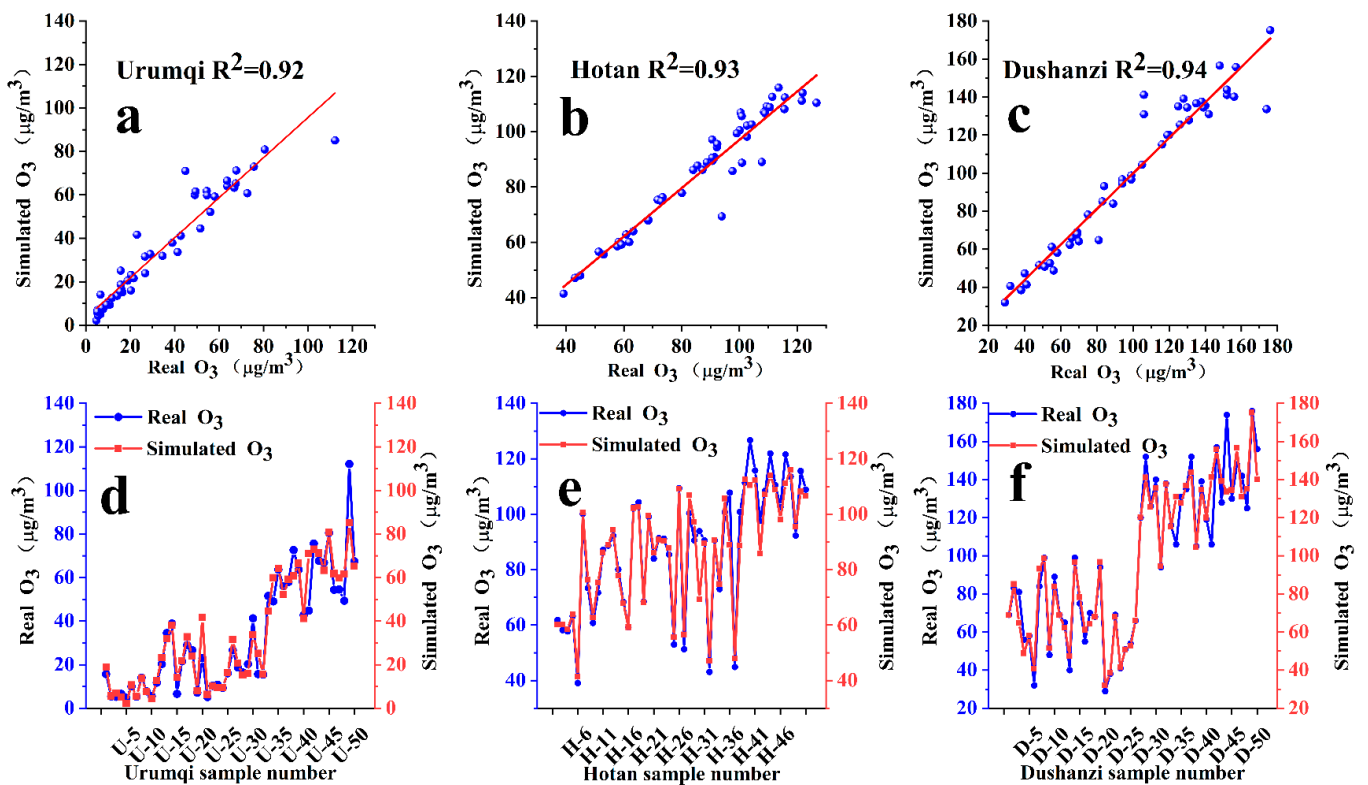


**Figure 4.** GA-BP artificial neural network model simulation results. (a) Results of linear fitting between real and simulated ozone values in Urumqi City. (b) Results of linear fitting between real and simulated ozone values in Hotan City. (c) Results of linear fitting between real and simulated ozone values in Dushanzi District. (d) Comparison of real and simulated ozone values in Urumqi City. (e) Comparison of real and simulated ozone values in Hotan City. (f) Comparison of real and simulated ozone values in Dushanzi District.

### 3.2. Results of the Ozone Concentration in Hotan City

As can be seen from Table S3, the relative error of the ozone simulation model based on the GA-BP neural network in Hotan City was  $4.2 \times 10^{-3}\%$  at minimum, 26.16% at maximum, and 4.39% at average after the simulation of the ozone concentration values of the 50-day samples in this area. The minimum absolute error was  $3.8 \times 10^{-3}$ , the maximum was 24.52, and the mean was 3.94. Among them, the number of days with a relative error of less than 30% was 50 days, accounting for 100%, and the number of days with a relative error of more than 50% was 0 days, accounting for 0%. The linear fitting results of the real value and simulated value of the ozone simulation model in Hotan City are shown in Figure 4b. The coefficient of determination for the linear fit between the real ozone concentration value and the simulated ozone concentration value was  $R^2 = 0.926$ . Figure 4e shows the comparison result of the ozone concentration value simulated by the Hotan model and the real ozone concentration value.

### 3.3. Results of the Ozone Concentration in Dushanzi District

As can be seen from Table S4, the ozone simulation model of the Dushanzi District based on the GA-BP neural network has a minimum relative error of  $2.4 \times 10^{-3}\%$  and a maximum of 33.2% after simulating the ozone concentration of 50-day samples in this area. The minimum absolute error was 0.016, the maximum was 40.32, and the mean was 5.80. Among them, the relative error was less than 30% for 49 days, accounting for 98%, and the relative error was more than 50% for 0 days, accounting for 0%. The linear fitting results of the true and simulated values of the ozone simulation model in the Dushanzi District are shown in Figure 4c. The coefficient of determination for the linear fit between the real ozone concentration value and the simulated ozone concentration value was  $R^2 = 0.935$ .

Figure 4f shows the comparison result of the ozone concentration value simulated by the Dushanzi model and the real ozone concentration value.

### 3.4. Comparison of the Simulation Results

To investigate whether the simulation results of the genetic algorithm optimized BP neural network (GA-BP) used in this study are accurate enough, the simulation results are compared with those of ordinary BP neural networks, traditional methods (MLR), random forest models (RF), and long- and short-term memory neural network models (LSTM). The performance parameters of all the models are shown in Table 4. The results showed that the errors (MAE, MSE, RMSE, and NRMSE) of the simulation results of the GA-BP neural network model were smaller than those of the other four simulation methods (BP, MLR, RF, and LSTM) in the Urumqi, Hotan, and Dushanzi districts.

**Table 4.** Performance metrics of the genetic algorithm optimized artificial neural network (GA-BP) compared with four other simulation methods (BP, MLR, RF, and LSTM).

		R <sup>2</sup>	MAE	MSE	RMSE	NRMSE
Urumqi City	GA-BP	0.92	4.31	54	7.34	0.07
	BP	0.72	10.0	180	13.4	0.13
	MLR	0.67	15.5	378	19.4	0.18
	RF	0.85	6.8	98.7	9.9	0.09
	LSTM	0.78	9.7	141	11.8	0.11
Hotan City	GA-BP	0.93	3.94	41	6.37	0.07
	BP	0.65	9.93	177	13.3	0.15
	MLR	0.62	10.0	191	13.8	0.16
	RF	0.80	7.7	101	10.1	0.12
	LSTM	0.74	8.5	132.7	11.5	0.13
Dushanzi District	GA-BP	0.94	5.80	102	10.1	0.07
	BP	0.83	14.3	304	17.5	0.12
	MLR	0.73	17.4	429	20.7	0.14
	RF	0.88	11.0	180	13.4	0.09
	LSTM	0.85	12.2	233	15.3	0.10

Note:  $p < 0.05$ .

As shown in the table, the coefficient of determination of the GA-BP neural network model in Urumqi (0.92) was much higher than that of the traditional simulation method (0.67), the ordinary BP neural network model (0.72), the random forest model (0.85), and the long- and short-term memory neural network model (0.78). The same results were found in the Hotan and Dushanzi regions, i.e., the R<sup>2</sup> of the GA-BP neural network model was higher than the other four simulation methods (BP, MLR, RF, and LSTM) in all three regions. Since the GA algorithm optimizes the weights and thresholds of the BP neural network model, the performance of GA-BP is improved compared to that of BP. Among these benchmark models—BP, MLR, LSTM, and RF—RF has the best simulation performance due to the fact that the model can perform random sampling of features and data and is not prone to overfitting. Among the three regions, because Urumqi is in an urban area, the anthropogenic influence is the largest and the factors affecting ozone generation are the most complex, which led to a lower fitting effect of the model in Urumqi compared to the remaining two cities among the three regions, when using the same model. The linear fitting results of all the simulation methods are shown in Figure 5. All the performance parameters of the GA-BP neural network were better than the other four methods, so the simulation results of the GA-BP neural network for ozone concentration were more accurate than the other four methods.

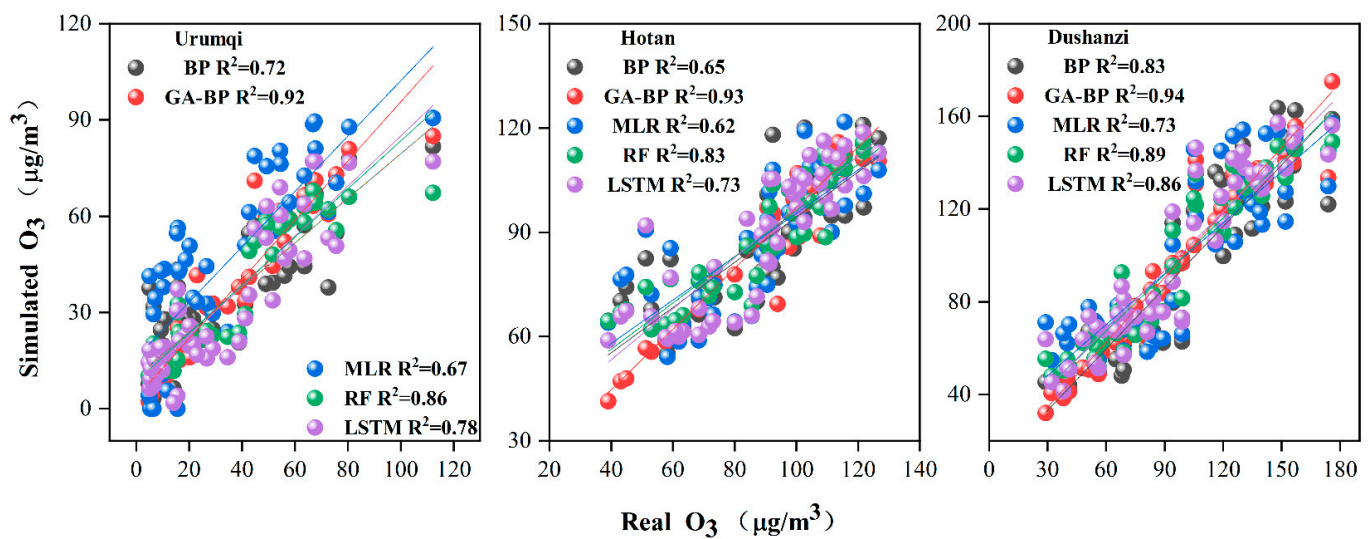


**Figure 5.** Determination coefficients ( $R^2$ ) of simulated  $O_3$  and real  $O_3$  by the GA-BP artificial neural network with four other methods (BP, MLR, RF, and LSTM) in Urumqi, Hotan, and Dushanzi districts.

### 3.5. Simulation Application of Three Models

We randomly generated 100 sets of meteorological parameter data and atmospheric condition data based on the real data of the three regions in the past to simulate the real situation of 100 days as realistically as possible. These 100 sets of meteorological parameter data and atmospheric condition data were within the range of common meteorological factors in the three regions and were close to the real meteorological conditions and atmospheric conditions. Using the controlled variable method and the same 100 sets of meteorological parameters through the simulation of different ozone simulation models in three regions, different ozone concentration simulation values were obtained. The simulated results of the three regions are shown in Figure 6. The specific simulated values are shown in Table S5. In a total of 100 samples, the results of the Urumqi City simulation model showed that the highest simulated ozone concentration was  $173.5 \mu\text{g}/\text{m}^3$  and the concentrations over 3 days exceeded the national standard second-level concentration limit ( $160 \mu\text{g}/\text{m}^3$ ). The results of the simulation model of Hotan City showed that the highest simulated ozone concentration was  $114.3 \mu\text{g}/\text{m}^3$ . The results of the simulation model of Dushanzi District showed that the highest simulated ozone concentration was  $228.4 \mu\text{g}/\text{m}^3$ . Shockingly, the national standard for secondary concentrations was exceeded on 14 of the 100 days in this simulation. According to the simulation model, the state of ozone pollution in Dushanzi District was relatively serious, which should arouse the attention of our society. Precursor emissions, atmospheric photochemical reactions, and atmospheric and meteorological factors jointly influence ozone production. The model was constrained in that the three regions were under the same meteorological and atmospheric conditions, but the precursor emissions in the three regions were different and the ozone pollution in Dushanzi district was more severe than that in Hotan and Urumqi, due to the large amount of VOCs and NO<sub>x</sub> emitted from industrial production in the Dushanzi district. This study suggests that the Dushanzi government should control the ozone precursor emissions to reduce ozone pollution.

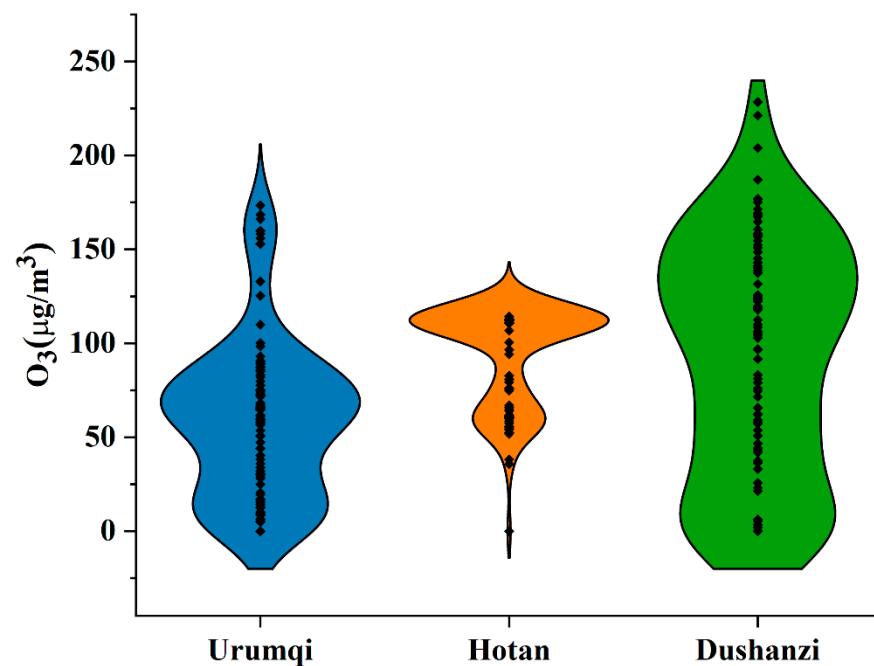


**Figure 6.** Simulation of ozone in the three regions of Xinjiang (Urumqi City, Dushanzi District, and Hotan City).

### 3.6. Limitations and the Next Research Plan

In this study, a BP neural network model optimized by a genetic algorithm was used to simulate ozone concentrations in three regions (Urumqi, Hotan, and Dushanzi districts) in Xinjiang, China. It is important to note that the model in this study still has some limitations and there are some areas for improvement. First, in this study, five meteorological factors and atmospheric conditions data were selected to simulate ozone concentrations and precursors of ozone (VOCs and NO<sub>x</sub>) were not used as input data for the model. While this improves the ease of operation and allows ozone concentrations to be simulated from the data provided by weather forecasts alone, the simulation performance of the model is not as accurate as a model that also includes precursor concentrations as inputs. Second, since this study is a preliminary attempt at a neural network model for simulating ozone concentration in the Xinjiang region, the comparison with other benchmark models is lacking. For example, the model built in this study is a single hidden-layer model optimized by a genetic algorithm and there is no comparison between the single-hidden layer model and the multi-hidden layer model; this study compares the simulation results of the GA-BP neural network model with an ordinary neural network model and traditional methods, but it still lacks the comparison between the simulation performance with other types of neural network architectures.

To address these shortcomings, we will reconsider the variables of the model inputs and, further, explore the accuracy differences of different types of neural network architectures in ozone concentration simulation tasks in the future.

## 4. Conclusions

After simulating and comparing the ozone concentration values in three regions of Xinjiang using the GA-BP neural network, the following conclusions were reached.

- (1) The simulation results of the GA-BP neural network model outperformed those of the BP, MLR, RF, and LSTM models in terms of accurately analyzing the relationships between the five input data categories (temperature, humidity, wind speed, wind direction, and visibility) and output data (ozone concentration). The GA-BP neural network was better fitted because the weights and thresholds of the BP neural network were optimized by the genetic algorithm. Among the three regions, Urumqi has

the largest anthropogenic influence and the most complex factors affecting ozone generation because it is in an urban area, which leads to the largest relative error (16%) in the model of Urumqi, among the three regions. The  $R^2$  values between the real and simulated ozone concentrations in Urumqi were 0.92, 0.93, and 0.94 in the Hotan and Dushanzi districts, respectively. This result indicates that the GA-BP neural network model is more suitable for ozone concentration simulation in urban areas, dusty areas, and industrial areas in Xinjiang, China. The ozone concentration simulation model constructed by the artificial GA-BP neural network has good generalization ability, high generality, and good objectivity and has practical application value.

- (2) Under the same wind speed, humidity, visibility, temperature, and wind direction, the ozone concentration data output from the GA-BP neural network models in the Urumqi, Hotan, and Dushanzi districts were significantly different. The highest simulated values of ozone concentration were the Dushanzi District ( $228.4 \mu\text{g}/\text{m}^3$ ) > Urumqi City ( $173.5 \mu\text{g}/\text{m}^3$ ) > Hotan City ( $114.3 \mu\text{g}/\text{m}^3$ ). In terms of the number of exceedance days, the ranking of exceedance days within 100 days was Dushanzi District (14 days) > Urumqi City (3 days) > Hotan City (0 days). Under the same meteorological and atmospheric conditions, the ozone concentrations in Dushanzi were at greater risk of pollution than in Hotan and Urumqi. This is because the Dushanzi district is an industrial area and factories in the area emit a large amount of the precursors (VOCs and NO<sub>x</sub>) needed to generate ozone, causing more serious ozone pollution in the area. Urumqi city also needs to be alerted to the ozone problem because of the high anthropogenic emissions of precursors in the urban area and the topographic factors limiting the dispersion of pollutants due to the mountains on three sides. In the Hotan city area, due to the higher wind speed, pollutants are more easily diffused; therefore, the problem of ozone pollution is less severe. It is recommended that the Dushanzi District should adopt emission reduction measures to reduce VOC and NO<sub>x</sub> emissions and ozone pollution in the area.

In the case of this study, meteorological factor data from three different functional areas in Xinjiang are selected for training and a GA-BP neural network is built for simulating the ozone concentration. If other regions are targeted, local data need to be used for training to obtain a suitable local model. Because the GA-BP neural network still has potential for improvement, in future studies, we will add variables to the model inputs and further delve into the accuracy of different types of neural network architectures in ozone concentration simulations.

**Supplementary Materials:** The following supporting information can be downloaded at: <https://www.mdpi.com/article/10.3390/atmos14010160/s1>, Table S1: Basic characteristics of the three regions; Table S2. Specific values of ozone prediction ( $\mu\text{g}/\text{m}^3$ ) in Urumqi City; Table S3. Specific values of ozone prediction ( $\mu\text{g}/\text{m}^3$ ) in Hotan City; Table S4. Specific values of ozone prediction ( $\mu\text{g}/\text{m}^3$ ) in Dushanzi District; Table S5. Specific values of ozone prediction in the three regions of Xinjiang (Urumqi City, Hotan City, and Dushanzi District).

**Author Contributions:** Conceptualization, K.J.; Methodology, K.J.; Software, K.J.; Validation, X.W.; Resources, A.A.; Data curation, X.Z. and B.L.; Writing—original draft, Q.Z.; Writing—review & editing, D.T. and B.G. All authors have read and agreed to the published version of the manuscript.

**Funding:** This study was supported by the National Natural Science Foundation of China (No. 41967050/41403093), Guangdong Natural Science Foundation (2015A030313868), Guangzhou Science and Technology Project (No. 201707010378).

**Institutional Review Board Statement:** Not applicable.

**Informed Consent Statement:** Not applicable.

**Data Availability Statement:** Data sharing is not applicable to this article.

**Acknowledgments:** Sincere thanks to all authors for their collaboration and fund support.

**Conflicts of Interest:** The authors declare no competing financial interest.

## References

1. Canella, R.; Roberta, B.; Cavicchio, C.; Cervellati, F.; Martini, M.; Muresan, X.M.; Valacchi, G. Tropospheric ozone effects on chlorine current in lung epithelial cells: An electrophysiological approach. *Free. Radic. Biol. Med.* **2016**, *96*, S58–S59. [[CrossRef](#)]
2. U.S. EPA. *Health Risk and Exposure Assessment for Ozone Final Report*; U.S. Environmental Protection Agency: Washington, DC, USA, 2014.
3. Rider, C.F.; Carlsten, C. Air pollution and DNA methylation: Effects of exposure in humans. *Clin. Epigenetics* **2019**, *11*, 131. [[CrossRef](#)] [[PubMed](#)]
4. Jin, T.; Xin, Y.; Yin, X.; Qi, J.; Wang, Y.; Han, M.; Zhao, S. Atmospheric ozone: Natural distribution, formation potential and effects on health: A review. *Sci. Technol. Rev.* **2018**, *36*, 39–47.
5. Fu, T.M.; Tian, H. Climate Change Penalty to Ozone Air Quality: Review of Current Understandings and Knowledge Gaps. *Curr. Pollut. Rep.* **2019**, *5*, 159–171. [[CrossRef](#)]
6. Simpson, D.; Arneth, A.; Mills, G.; Solberg, S.; Uddling, J. Ozone—The persistent menace: Interactions with the N cycle and climate change. *Curr. Opin. Environ. Sustain.* **2014**, *9–10*, 9–19. [[CrossRef](#)]
7. Aiping, D.; Weiqing, L.; Xue, Y.; Center, J.E.M. Analysis on Change of Primary Pollutant in Ambient Air of Jiangsu Province during 2013 and 2017. *Environ. Sci. Manag.* **2017**, *12*, 19–22.
8. Shen, J.; Huang, X.; Wang, Y.; Ye, S.; Pan, Y.; Chen, D.; Chen, H.; Ou, Y.; Lu, X.; Wang, Z. Study on ozone pollution characteristics and source apportionment in Guangdong Province. *Acta Sci. Circumst.* **2017**, *37*, 4449–4457.
9. Li, K.; Jacob, D.J.; Liao, H.; Shen, L.; Zhang, Q.; Bates, K.H. Anthropogenic drivers of 2013–2017 trends in summer surface ozone in China. *Proc. Natl. Acad. Sci. USA* **2019**, *116*, 422–427. [[CrossRef](#)]
10. Feng, Z.; Li, P.; Yuan, X.; Gao, F.; Jiang, L.; Dai, L. Progress in ecological and environmental effects of ground-level O<sub>3</sub> in China. *Acta Ecol. Sin.* **2018**, *38*, 1530–1541.
11. Liu, H.; Liu, S.; Xue, B.; Lv, Z.; Meng, Z.; Yang, X.; Xue, T.; Yu, Q.; He, K. Ground-level ozone pollution and its health impacts in China. *Atmos. Environ.* **2018**, *173*, 223–230. [[CrossRef](#)]
12. Brauer, M.; Freedman, G.; Frostad, J.; Van Donkelaar, A.; Martin, R.; Dentener, F.; Van Dingenen, R.; Estep, K.; Amini, H.; Apte, J.; et al. Ambient air pollution exposure estimation for the global burden of disease 2013. *Environ. Sci. Technol.* **2016**, *50*, 79–88. [[CrossRef](#)] [[PubMed](#)]
13. Li, T.; Yan, M.; Ma, W.; Ban, J.; Liu, T.; Lin, H.; Liu, Z. Short-term effects of multiple ozone metrics on daily mortality in a megacity of China. *Environ. Sci. Pollut. Res.* **2015**, *22*, 8738–8746. [[CrossRef](#)] [[PubMed](#)]
14. Anenberg, S.C.; Horowitz, L.W.; Tong, D.Q.; West, J.J. An estimate of the global burden of anthropogenic ozone and fine particulate matter on premature human mortality using atmospheric modeling. *Environ. Health Perspect.* **2010**, *118*, 1189–1195. [[CrossRef](#)] [[PubMed](#)]
15. Bao, J.; Cao, J.; Gao, R.; Ren, Y.; Bi, F.; Wu, Z.; Chai, F.; Li, H. Process and Experience of Ozone Pollution Prevention and Control in Europe and Enlightenment to China. *Res. Environ. Sci.* **2021**, *34*, 890–901.
16. Worden, H.M.; Bowman, K.W.; Worden, J.R.; Eldering, A.; Beer, R. Satellite measurements of the clear-sky greenhouse effect from tropospheric ozone. *Nat. Geosci.* **2008**, *1*, 305–308. [[CrossRef](#)]
17. Silva, R.A.; West, J.J.; Zhang, Y.Q.; Anenberg, S.C.; Lamarque, J.F.; Shindell, D.T.; Collins, W.J.; Dalsoren, S.; Faluvegi, G.; Folberth, G.; et al. Global premature mortality due to anthropogenic outdoor air pollution and the contribution of past climate change. *Environ. Res. Lett.* **2013**, *8*, 034005. [[CrossRef](#)]
18. Chen, Y.; Beig, G.; Archer-Nicholls, S.; Drysdale, W.; Acton, W.J.F.; Lowe, D.; Nelson, B.; Lee, J.; Ran, L.; Wang, Y.; et al. Avoiding high ozone pollution in Delhi, India. *Faraday Discuss.* **2021**, *226*, 502–514. [[CrossRef](#)]
19. Fujita, E.M.; Campbell, D.E.; Stockwell, W.R.; Saunders, E.; Fitzgerald, R.; Perea, R. Projected ozone trends and changes in the ozone-precursor relationship in the South Coast Air Basin in response to varying reductions of precursor emissions. *J. Air Waste Manag. Assoc.* **2016**, *66*, 201–214. [[CrossRef](#)]
20. Calvert, J.G.; Orlando, J.J.; Stockwell, W.R.; Wallington, T.J. *The Mechanisms of Reactions Influencing Atmospheric Ozone*; Oxford University Press: Oxford, UK, 2015.
21. Wang, T.; Xue, L.; Brimblecombe, P.; Lam, Y.F.; Li, L.; Zhang, L. Ozone pollution in China: A review of concentrations, meteorological influences, chemical precursors, and effects. *Sci. Total Environ.* **2016**, *575*, 1582–1596. [[CrossRef](#)]
22. Xiao, X.; Cohan, D.S.; Byun, D.W.; Ngan, F. Highly nonlinear ozone formation in the Houston region and implications for emission controls. *J. Geophys. Res. Atmos.* **2010**, *115*, D23309. [[CrossRef](#)]
23. Li, G.-Y.; Chen, Q.; Guo, W.-K.; Zhang, R.-X.; Xia, J.-Q. Nonlinear Response Characteristics and Control Scheme for Ozone and Its Precursors Based on Orthogonal Experimental Methods. *Huan Jing Ke Xue* **2021**, *42*, 616–623. [[CrossRef](#)] [[PubMed](#)]
24. Dong, Y.; Li, J.; Guo, J.; Jiang, Z.; Liao, H. The impact of synoptic patterns on summertime ozone pollution in the North China Plain. *Sci. Total Environ.* **2020**, *735*, 139559. [[CrossRef](#)]
25. Putra, J.C.P.; Safrilah; Ihsan, M. The Prediction of Indoor Air Quality in Office Room Using Artificial Neural Network. In Proceedings of the 4th International Conference on Engineering, Technology, and Industrial Application (ICETIA), Surakarta, Indonesia, 13–14 December 2017.
26. Lei, L.; Chen, W.; Xue, Y.; Liu, W. A comprehensive evaluation method for indoor air quality of buildings based on rough sets and a wavelet neural network. *Build. Environ.* **2019**, *162*, 106296. [[CrossRef](#)]

27. Huang, Y.; Xiang, Y.X.; Zhao, R.X.; Cheng, Z. Air Quality Prediction Using Improved PSO-BP Neural Network. *IEEE Access* **2020**, *8*, 99346–99353. [[CrossRef](#)]
28. Du, S.D.; Li, T.R.; Yang, Y.; Horng, S.J. Deep Air Quality Forecasting Using Hybrid Deep Learning Framework. *IEEE Trans. Knowl. Data Eng.* **2021**, *33*, 2412–2424. [[CrossRef](#)]
29. Liao, Q.; Zhu, M.M.; Wu, L.; Pan, X.L.; Tang, X.; Wang, Z.F. Deep Learning for Air Quality Forecasts: A Review. *Curr. Pollut. Rep.* **2020**, *6*, 399–409. [[CrossRef](#)]
30. Wan, X.-L.; Yang, F.-L.; Wang, H.-Q. The approach of artificial neural network applied in ambient ozone forecast. *China Environ. Sci.* **2003**, *23*, 110–112.
31. Xing, J.; Zheng, S.; Li, S.; Huang, L.; Wang, X.; Kelly, J.T.; Wang, S.; Liu, C.; Jang, C.; Zhu, Y. Mimicking atmospheric photochemical modeling with a deep neural network. *Atmos. Res.* **2022**, *265*, 105919. [[CrossRef](#)]
32. Cheng, Y.; He, L.-Y.; Huang, X.-F. Development of a high-performance machine learning model to predict ground ozone pollution in typical cities of China. *J. Environ. Manag.* **2021**, *299*, 113670. [[CrossRef](#)]
33. Hur, S.K.; Oh, H.R.; Ho, C.H.; Kim, J.; Song, C.K.; Chang, L.S.; Lee, J.B. Evaluating the predictability of PM10 grades in Seoul, Korea using a neural network model based on synoptic patterns. *Environ. Pollut.* **2016**, *218*, 1324–1333. [[CrossRef](#)]
34. Biancofiore, F.; Busilacchio, M.; Verdecchia, M.; Tomassetti, B.; Aruffo, E.; Bianco, S.; Di Tommaso, S.; Colangeli, C.; Rosatelli, G.; Di Carlo, P. Recursive neural network model for analysis and forecast of PM10 and PM2.5. *Atmos. Pollut. Res.* **2017**, *8*, 652–659. [[CrossRef](#)]
35. Eslami, E.; Choi, Y.; Lops, Y.; Sayeed, A. A real-time hourly ozone prediction system using deep convolutional neural network. *Neural Comput. Appl.* **2019**, *32*, 8783–8797. [[CrossRef](#)]
36. Adnan, R.M.; Mostafa, R.R.; Islam, A.R.M.T.; Kisi, O.; Kuriqi, A.; Heddad, S. Estimating reference evapotranspiration using hybrid adaptive fuzzy inferencing coupled with heuristic algorithms. *Comput. Electron. Agric.* **2021**, *191*, 106541. [[CrossRef](#)]
37. Adnan, R.M.; Kisi, O.; Mostafa, R.R.; Ahmed, A.N.; El-Shafie, A. The potential of a novel support vector machine trained with modified mayfly optimization algorithm for streamflow prediction. *Hydrol. Sci. J.* **2022**, *67*, 161–174. [[CrossRef](#)]
38. Adnan, R.M.; Mostafa, R.R.; Elbeltagi, A.; Yaseen, Z.M.; Shahid, S.; Kisi, O. Development of new machine learning model for streamflow prediction: Case studies in Pakistan. *Stoch. Environ. Res. Risk Assess.* **2022**, *36*, 999–1033. [[CrossRef](#)]
39. Grefenstette, J.J. Genetic Algorithms and Machine Learning. *Mach. Learn.* **1988**, *3*, 95–99. [[CrossRef](#)]
40. Song, Y.; Wang, F.; Chen, X. An improved genetic algorithm for numerical function optimization. *Appl. Intell.* **2019**, *49*, 1880–1902. [[CrossRef](#)]
41. Hong, H.; Panahi, M.; Shirzadi, A.; Ma, T.; Liu, J.; Zhu, A.-X.; Chen, W.; Kougiaris, I.; Kazakis, N. Flood susceptibility assessment in Hengfeng area coupling adaptive neuro-fuzzy inference system with genetic algorithm and differential evolution. *Sci. Total Environ.* **2018**, *621*, 1124–1141. [[CrossRef](#)]
42. Seyedpour, S.; Kirmizakis, P.; Brennan, P.; Doherty, R.; Ricken, T. Optimal remediation design and simulation of groundwater flow coupled to contaminant transport using genetic algorithm and radial point collocation method (RPCM). *Sci. Total Environ.* **2019**, *669*, 389–399. [[CrossRef](#)]
43. Huang, J.; Zhu, Y.; Kelly, J.T.; Jang, C.; Wang, S.; Xing, J.; Chiang, P.-C.; Fan, S.; Zhao, X.; Yu, L. Large-scale optimization of multi-pollutant control strategies in the Pearl River Delta region of China using a genetic algorithm in machine learning. *Sci. Total Environ.* **2020**, *722*, 137701. [[CrossRef](#)]
44. Zhang, X.X.; Ding, X.; Talifu, D.; Wang, X.M.; Abulizi, A.; Maihemuti, M.; Rekefu, S. Humidity and PM2.5 composition determine atmospheric light extinction in the arid region of northwest China. *J. Environ. Sci.* **2021**, *100*, 279–286. [[CrossRef](#)]
45. Turap, Y.; Talifu, D.; Wang, X.M.; Abulizi, A.; Maihemuti, M.; Tursun, Y.; Ding, X.; Aierken, T.; Rekefu, S. Temporal distribution and source apportionment of PM2.5 chemical composition in Xinjiang, NW-China. *Atmos. Res.* **2019**, *218*, 257–268. [[CrossRef](#)]
46. Liu, H.B.; Wang, X.M.; Talifu, D.; Ding, X.; Abulizi, A.; Tursun, Y.; An, J.Q.; Li, K.J.; Luo, P.; Xie, X.X. Distribution and sources of PM2.5-bound free silica in the atmosphere of hyper-arid regions in Hotan, North-West China. *Sci. Total Environ.* **2022**, *810*, 152368. [[CrossRef](#)]
47. Gupta, J.N.; Sexton, R.S. Comparing backpropagation with a genetic algorithm for neural network training. *Omega* **1999**, *27*, 679–684. [[CrossRef](#)]
48. Feng, Y.; Zhang, W.; Sun, D.; Zhang, L. Ozone concentration forecast method based on genetic algorithm optimized back propagation neural networks and support vector machine data classification. *Atmos. Environ.* **2011**, *45*, 1979–1985. [[CrossRef](#)]
49. Yu, S.; Guo, X.; Zhu, K.; Du, J. A neuro-fuzzy GA-BP method of seismic reservoir fuzzy rules extraction. *Expert Syst. Appl.* **2010**, *37*, 2037–2042. [[CrossRef](#)]
50. Huang, C.-Y.; Chen, L.-H.; Chen, Y.-L.; Chang, F.M. Evaluating the process of a genetic algorithm to improve the back-propagation network: A Monte Carlo study. *Expert Syst. Appl.* **2009**, *36*, 1459–1465. [[CrossRef](#)]
51. Jia, B.; Dong, R.; Du, J. Ozone concentrations prediction in Lanzhou, China, using chaotic artificial neural network. *Chemom. Intell. Lab. Syst.* **2020**, *204*, 104098. [[CrossRef](#)]
52. Özbay, B.; Keskin, G.A.; Doğruparmak, Ş.Ç.; Ayberk, S. Predicting tropospheric ozone concentrations in different temporal scales by using multilayer perceptron models. *Ecol. Inform.* **2011**, *6*, 242–247. [[CrossRef](#)]
53. Yao, M. Application of improved genetic algorithm in optimizing BP neural networks weights. *Comput. Eng. Appl.* **2013**, *49*, 49–54.
54. Li, X. A comparison between information transfer function sigmoid and tanh on neural. *J. Wuhan Univ. Technol* **2004**, *28*, 312–314.

55. Goudarzi, G.; Hopke, P.K.; Yazdani, M. Forecasting PM<sub>2.5</sub> concentration using artificial neural network and its health effects in Ahvaz, Iran. *Chemosphere* **2021**, *283*, 131285. [[CrossRef](#)] [[PubMed](#)]
56. Yafouz, A.; Ahmed, A.N.; Zaini, N.; Sherif, M.; Sefelnasr, A.; El-Shafie, A. Hybrid deep learning model for ozone concentration prediction: Comprehensive evaluation and comparison with various machine and deep learning algorithms. *Eng. Appl. Comput. Fluid Mech.* **2021**, *15*, 902–933. [[CrossRef](#)]

**Disclaimer/Publisher's Note:** The statements, opinions and data contained in all publications are solely those of the individual author(s) and contributor(s) and not of MDPI and/or the editor(s). MDPI and/or the editor(s) disclaim responsibility for any injury to people or property resulting from any ideas, methods, instructions or products referred to in the content.